PAPER REFERENCE: No: A2600

Hard Numbers on Soft Matter

H. Rydberg*, N. Jacobson*, P. Hyldgaard*, S.I. Simak*, B.I. Lundqvist*[1] and D.C. Langreth§

*Department of Applied Physics, Chalmers University of Technology and Göteborg University, S-412 96 Göteborg, Sweden

§Center for Materials Theory, Department of Physics and Astronomy, Rutgers University, Piscataway, New Jersey 08854-8019, USA.

Abstract

Graphitic systems are ideal examples of the soft-matter challenge for quantum mechanics that must account for both strong local atom bonds and weak nonlocal van der Waals interactions between atoms separated by empty space. Here a new density functional (DF), which encompasses nonlocal correlations among the electrons, is applied successfully to obtain structure, bonding, and compressibility, documenting the decisive role of the interlayer vdW interactions. The understanding emerging from this new extended-DF formulation has bearing on broad classes of problems, including surfaces, in physics, chemistry, biology, medicine, and technology, where we can now provide an efficient and accurate DF-theory account.

Keywords:

Construction and use of effective interatomic interactions, Density-functional calculations, Many-body theories, Chemisorption, Growth, Physical adsorption, Sticking, Surface energy.

[1]Corresponding author: Tel. +46 31 772 3198; Fax: +46 31 772 8426; E-mail: `lundqvist@fy.chalmers.se`

1. Introduction

Today, materials theory is a full-fledged partner in the development of new materials. Bonds, structures, and other properties come out impressively well, a clear success of the now "standard" version of density-functional theory (DFT). This has led to its use in a great variety of fields in physics, chemistry, and biology, including surface applications. The clearest success has been for dense and hard materials. Large-scale applications to sparse or soft matter, which occurs in many fields, but most prevalently in biological ones, have been less frequent. This is partly because of computational complexity, but perhaps mostly because the standard density functionals in use today do not and cannot capture the long range van der Waals or dispersion interactions, which are important in such systems. Much progress has been made in the former problem, which may be well under way toward solution. However, the latter problem has been resistant. Here we demonstrate through a key application of a new nonlocal density functional [1] to a classic sparse system, that this latter problem may be well under way to solution as well. Such a development should open up the full power of first-principle electronic-structure calculations to most all fields of natural science.

The present standard DFT applies so-called generalized-gradient approximations (GGA). It offers highly accurate descriptions of dense and hard materials, like metals, semiconductors, dielectric insulators, ionic crystals, ceramics, and magnets. One can determine bond lengths with an accuracy of 1 per cent [2], proper stable structures with an edge of about 30 meV/atom compared to competing structures [3, 4], diffusion barriers in crystal growth with an accuracy of about 10 meV [5], and compressibilities typically within 10 per cent of measured values [2]. A particular driving force for the development of improved density functionals (DFs) is its application to dense surfaces, where numerous accurate experimental techniques meet advanced theory and enable detailed comparisons on the quantum level [6].

For sparse and soft matter — a class of materials and molecular assemblies at least as abundant and important as the hard matter — standard DFT needs to be augmented. It meets a real challenge: to account for *both* strong intramolecular bonding *and* weak intermolecular dispersion forces. The latter has hitherto eluded most of the DFT studies. Being based on local (local-density approximation, LDA) and semilocal (GGA) electron correlations, the standard DFT omits key physical interactions and cannot, even in principle, provide consistent and accurate calculations for soft matter. The exact DFT includes a general description of all interactions [7], but the challenge is to provide an approximate DF that is universally applicable, *i.e.,* which also accounts for the nonlocal nature of the physical interactions. We have proposed successively more versatile functionals with such properties [8, 9, 10, 1], and so have others [11, 12, 13].

This report describes a successful large-system application of our new DF [1] and documents how a combination of local and nonlocal interactions provides a first accurate quantum-physical description of these text-book materials. The successful application to graphite and graphene (a single layer of graphite) and the recent implementation for arbitrary geometries [14] open the way for a revised DFT. Many important materials that are characterized by and, in fact, operate through the weak ubiquitous vdW interaction can now finally be accounted for within an accurate and computationally efficient quantum-mechanical description.

2. Applications to Graphitic Systems

We choose graphite and graphene for our study of soft matter because of their simplicity and juxtaposition with diamond, another solid composed solely of the element carbon. Whereas graphite is one of the softest minerals, diamond is the hardest; graphite is opaque and black, while pure diamond is transparent and colorless; and graphite is a conductor, while diamond is an insulator. Graphite's technological importance also provides a motivation. Applications include fuel cells, sealing materials, powdered metallurgy, friction products, shapes, steel-mill and foundry products, lubricants, and plastics, not to mention pencils. The prime reason for choosing graphitic systems, however, is the textbook-sharp distinction between regions of covalent and van der Waals bonding, respectively, in these systems. A working DFT has to account for *both* the strong local bonds between atoms within the layers *and* the weak nonlocal bonds between layers of atoms separated by empty space.

The structure of graphite is that of a staggered stacking of flat layers of carbon atoms a distance $d^{\mathrm{exp}} \approx 3.35$ Å apart [15] (Fig. 1). Individual layers, referred to as "graphene" sheets [16], are composed of strongly bonded carbon atoms, situated at the vertices of a network of regular hexagons of side $a/\sqrt{3}$, forming a honeycomb pattern with lattice constant $a^{\mathrm{exp}} \approx 2.46$ Å [17]. Graphene is materialized in nature, for example in collapsed carbon nanotubes [18] and on surfaces [19]. In graphite, the graphene layers are weakly bonded to each other.

It is surprising that the public discussion of the problems encountered when applying standard (semilocal) DFT to graphitic systems has been limited and contradictory [20, 21, 22]. This precarious situation may be due to the fact that for a long period, the early (LDA) version of DFT was repeatedly shown to give reasonable predictions at equilibrium separations [23, 24, 25, 26, 22], thus obscuring the fortuitousness of this result and providing demotivation for further work. In this report we document (i) a strong disagreement between the early DFT (LDA) results and experiment for graphite, (ii) the complete breakdown of the current standard DFT (GGA) for soft matter, and (iii) the successful application of our recent nonlocal DFT [1], which accounts for van der Waals interactions, and which yields excellent agreement with experimental results on structure, bonding, and compressibility, not the least important for soft matter (Similar conclusions have been drawn for the intermediate interactions of benzene [27], however with an empirical account [28] for the vdW interactions.

First the binding-energy curve of two parallel graphene sheets is calculated, *i.e.,* the difference in the total-energy values at separation d and at infinite separation, respectively, for varying d (Fig. 2). The standard-DFT curve is completely wrong, lacking any indication of van der Waals effects [29], as it should. With our "revised-DFT" method, which embodies our van der Waals correction, a binding-energy value of 34 (35 ± 10) meV/atom at the equilibrium interplanar distance 3.5 (3.35) Å is obtained in the ABAB stacking, where the values within parenthesis are experimental numbers, obtained from collapsed carbon nanotubes [18].

The second application is on graphite whose calculated total energy $E(c, a)$ is shown in Fig. 3 as energy contours in the c–a plane. The standard-DFT (GGA) result in the left panel documents that it gives unphysical results. Its minimum, if any, appears for $c \gg 3a$. Experimentally, $2.7 \leq c^{\mathrm{exp}}/a^{\mathrm{exp}} \leq 2.73$ [15]. The revised-DFT energy contours look much more physical (right panel), giving a potential-energy minimum of 34 meV/atom at the equilibrium interplanar distance $c = 2.85a$. The binding-energy curve for varying lattice constant c differs negligibly from that for two parallel graphene sheets.

The concept of softness gets ample illustration by the bulk-modulus values shown in Table 1. For graphite, the early-standard DFT (LDA) gives a value for the bulk modulus that is too high, and the current standard (GGA) gives too low a value, while the revised form (nonlocal DF) gives a value in close agreement with experiment (33 GPa) [30] (As a comparison, the diamond values are close to each other and one order of magnitude higher, 440 GPa.).

3. Conclusion

In summary, with the key examples of two interacting graphene sheets and of graphite, the standard DFT (GGA) is shown not to be applicable for calculating properties of soft matter. Use of our van der Waals DF [1] seems to be one way to proceed. As the outcome is so positive, we judge that we have in our hands the first practically working version of such a functional [1]. Together with increased efficiency in DFT calculations this gives promise for a broad range of applications in soft matter, *i.e.* to the sparse systems that define most physical, chemical, and biological phenomena, *e.g.,* biomacromolecules, biosurfaces, polymers, liquid crystals, membranes, mica, ski wax, lubrication, physisorption, adhesion, and interacting organic molecules. In particular, there is a range of key surface phenomena within reach.

4. Acknowledgements

This work has been supported by the Swedish Research Council, the Swedish Foundation for International Cooperation in Research and Higher Education (STINT), and the Swedish Foundation for Strategic Research (SSF) through the materials consortia no. 9 and ATOMICS. Work by DCL supported in part by the NSF (USA) under grant DMR 00-93079.

References:

[1] Rydberg, H., Lundqvist, B. I., Langreth, D. C. & Dion, M. *Phys. Rev. B* **62**, 6997–7006 (2000).

[2] Kurth, S., Perdew, J. P. & Blaha, P. *Int. J. Quantum. Chem.* **75**, 889–909 (1999).

[3] Häglund, J. *Phys. Rev. B* **47**, 566–569 (1993).

[4] Yourdshahyan, Y. *et al. J. Am. Ceram. Soc.* **82**, 1365–1380 (1999).

[5] Bogicevic, A., Strömqvist, J. & Lundqvist, B. I. *Phys. Rev. Lett.* **81**, 637–640 (1998).

[6] Lundqvist, B. I. *et al. Surface Science* **493**, 253–270 (2001).

[7] Lundqvist, B. I., Andersson, Y., Shao, H., Chan, S., & Langreth, D. C. *Int. J. Quantum. Chem* **56**, 247–255 (1995).

[8] Andersson, Y., Langreth, D. C. & Lundqvist, B. I. *Phys. Rev. Lett.* **76**, 102–105 (1996).

[9] Hult, E., Andersson, Y., Lundqvist, B. I. & Langreth, D. C. *Phys. Rev. Lett.* **77**, 2029–2032 (1996).

[10] Hult, E., Rydberg, H., Lundqvist, B. I. & Langreth, D. C. *Phys. Rev. B* **59**, 4708–4713 (1998).

[11] Dobson, J. F. & Dinte, B. P. *Phys. Rev. Lett.* **76**, 1780–1783 (1996).

[12] Kohn, W., Meir, Y. & Makarov, D. E. *Phys. Rev. Lett.* **80**, 4153–4156 (1998).

[13] Dobson, J. F. & Wang, J. *Phys. Rev. Lett.* **82**, 2123–2126 (1999).

[14] Rydberg, H. Ph D. Thesis (2001), ISBN 91-7291-068-2.

[15] Baskin, Y. & Mayer, L. *Phys. Rev.* **100**, 544–544 (1955).

[16] Dresselhaus, M. S., Dresselhaus, G., Surihara, K., Spain, I. L. & Goldberg, H. A. *Graphite Fibers and Filaments* (Springer, Berlin, 1988).

[17] Freise, E. J. *Nature* **193**, 671–672 (1962).

[18] Benedict, L. X. *et al. Chem. Phys. Lett.* **286**, 490–496 (1998).

[19] Forbeaux, I., Themlin, J.-M. & Debever, J.-M. *Phys. Rev. B* **58**, 16396–16406 (1998).

[20] Kganyago, K. R. & Ngoepe, P. E. *Molecular Simulation* **22**, 39–43 (1999).

[21] Lee, I.-H. & Martin, R. M. *Phys. Rev. B* **56**, 7197–7205 (1997).

[22] Kern, G. & Hafner, J. *Phys. Rev. B* **58**, 13167-13175 (1998).

[23] Yin, M. T. & Cohen, M. L. *Phys. Rev. B* **29**, 6996–6998 (1984).

[24] Jansen, H. J. F. & Freeman, A. J. *Phys. Rev. B* **35**, 8207–8214 (1987).

[25] Schabel, M. C. & Martins, J. L. *Phys. Rev. B* **46**, 7185–7188 (1992).

[26] Charlier, J. C., Gonze, X. & Michenaud, J. P. *Europhys. Lett.* **28**, 403–408 (1994).

[27] Meijer, E. J., and Sprik, M., *J. Chem. Phys.* **105**, 8684–8689 (1996).

[28] Yashonath, S., Price, S. L., and McDonald, I. R., *Mol. Phys.* **64**, 361 (1988).

[29] Patton, D. C. & Pederson, M. R. *Phys. Rev. A* **56**, R2495–R2498 (1997).

[30] Beggerow, G. *Landolt-Börnstein*, Vol. IV/4 (Springer, Berlin, 1980).

[31] Hansen, L. B. *et al.* Computer code **dacapo-1.30**. *The Center for Atomic-Scale Materials Physics (CAMP)*, Technical University of Denmark, Lyngby, Denmark.

[32] Perdew, J. P. in *Electronic Structure of Solids '91* (eds Ziesche, P. & Eschrig, H.) 11–20 (Akademie Verlag, Berlin, 1991).

[33] Kohn, W. & Sham, L. J. *Phys. Rev.* **140**, A1133-A1138 (1965).

[34] In Ref. [1] the approximation for this nonlocal functional is described as 'RPA-like', a description that is here clarified: The RPA consists in setting the coupling constant $\lambda = 0$ in the $\tilde{\chi}$ of Eq. (2) in Ref. [1] before the coupling-constant integral is done. What we do is to set $\lambda = 1$ in $\tilde{\chi}$ before the coupling constant integral is done. The former approximation neglects the beyond-RPA terms entirely, while the latter includes them too strongly, although both give equations with the same formal RPA-like appearance. The static polarization properties of $\tilde{\chi}$ in our approximation are controlled by the parameter $q_{\perp}$, whose value is computed from a full standard GGA calculation, not the RPA version of the LDA or GGA. Since the static polarizability is calculated as a self-consistent ground state property, the polarization response to the change in the exchange-correlation potential induced by the field is automatically included, while in an RPA calculation, only the direct or Hartree polarization response to the field would be included.

[35] Hult, E. , Hyldgaard, P, Rossmeisl, J, and Lundqvist, B. I. *Phys. Rev. B* **64**, 195414-1–7 (2001).

[36] Kresse, G. & Joubert, J. *Phys. Rev. B* **59**, 1758–1775 (1999).

[37] Lee, I.-H. & Martin, R. M. *Phys. Rev. B* **56**, 7197–7205 (1997).

FIGURE CAPTIONS

Figure 1: The hexagonal layered structure of graphite. The intraplanar ($a/\sqrt{3}$) bondlength (adjacent atoms in foreground) is shorter than in diamond, whereas the interplanar ($d = c/2$) bondlength (distance between adjacent layers) is large. As a consequence, the electronic overlap between the layers is small. Standard DFT estimates the many-body effects from this small overlap only, whereas the physical interaction is *between* the layers, explaining the inability of standard DFT to properly account for the bonding.

Figure 2: The binding energy of a single graphene-graphene pair as a function of interplanar separation (d), presented in units of a periodic (graphite) system. A pseudopotential code [31] and a semilocal approximation [32] are used to calculate the standard-DFT electron densities, $n_d(\mathbf{r})$, and energies, for each separation d. The exchange part of the new functional is unchanged from standard DFT, while the correlation part [1] is easily related to it. The standard correlation functional can be written as $E_{\rm c}^{\rm standard} = E_{\rm c}^{\rm LDA} + E_{\rm c}^{\rm semilocal}$ where $E_{\rm c}^{\rm LDA}$ is the old-standard or local-density approximation [33] contribution and $E_{\rm c}^{\rm semilocal}$ is the semilocal correction. Correspondingly, our new correlation functional [34] may be written $E_{\rm c}^{\rm new} = E_{\rm c}^{\rm LDA} + E_{\rm c}^{\rm nonlocal}$, where $E_{\rm c}^{\rm nonlocal}$ is our replacement, which although fully nonlocal, is calculationally inexpensive. It is calculated using Eqs. (9), (19) and (23) of Ref. [1] with laterally averaged densities $n_d(z)$ as input (The relevant density is out in the tails of the electron density of each layer [35]. It is smooth, making the corrugation negligible compared with the separation between the fragments). The system-specific component ($q_\perp$) is kept fixed for all separations d. It is determined by comparing a (standard DFT) calculation of the static polarizability (actually α_{zz}, where the z direction is perpendicular to the graphene plane) of a single graphene sheet to the classical electrodynamic formulation.

Figure 3: *Left panel:* Total-energy contour plot for graphite in the c–a plane, calculated with standard DFT. The energy is increasing in order darker to lighter shades of grey with a 10 meV contour spacing. The lattice parameters are defined in Fig. 1. An all-electron projector augmented-wave method [36] and a semilocal approximation [32] are used. The dashed curve is the locus of points giving the experimental volume; it illustrates that a calculation so constrained will fortuitously give the correct values of c and a [37]. *Right panel:* Same system calculated with our nonlocal-correlation corrected DFT, as described in Fig. 2.

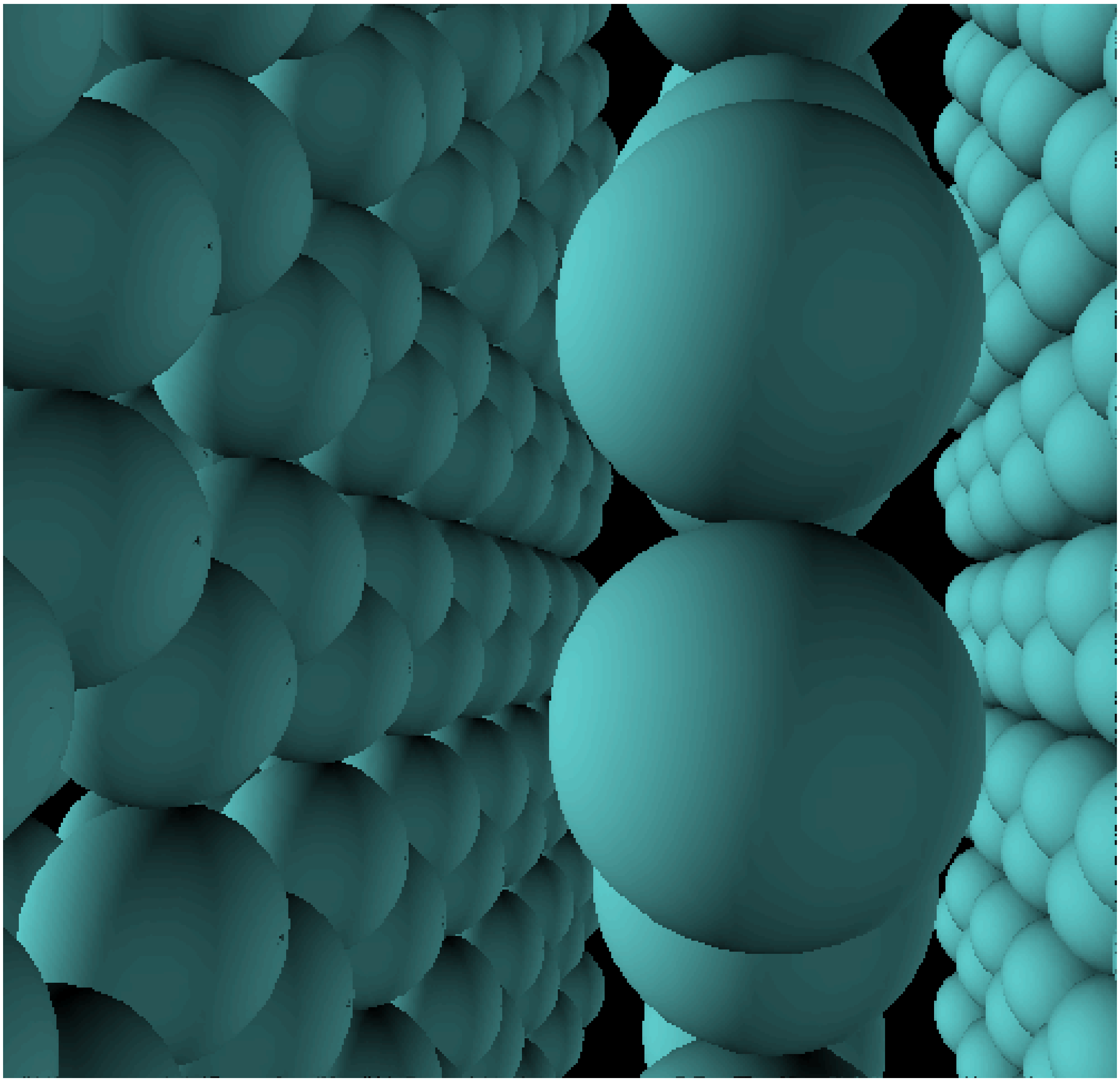

Figure 1: The hexagonal layered structure of graphite. The intraplanar ($a/\sqrt{3}$) bondlength (adjacent atoms in foreground) is shorter than in diamond, whereas the interplanar ($d = c/2$) bondlength (distance between adjacent layers) is large. As a consequence, the electronic overlap between the layers is small. Standard DFT estimates the many-body effects from this small overlap only, whereas the physical interaction is *between* the layers, explaining the inability of standard DFT to properly account for the bonding.

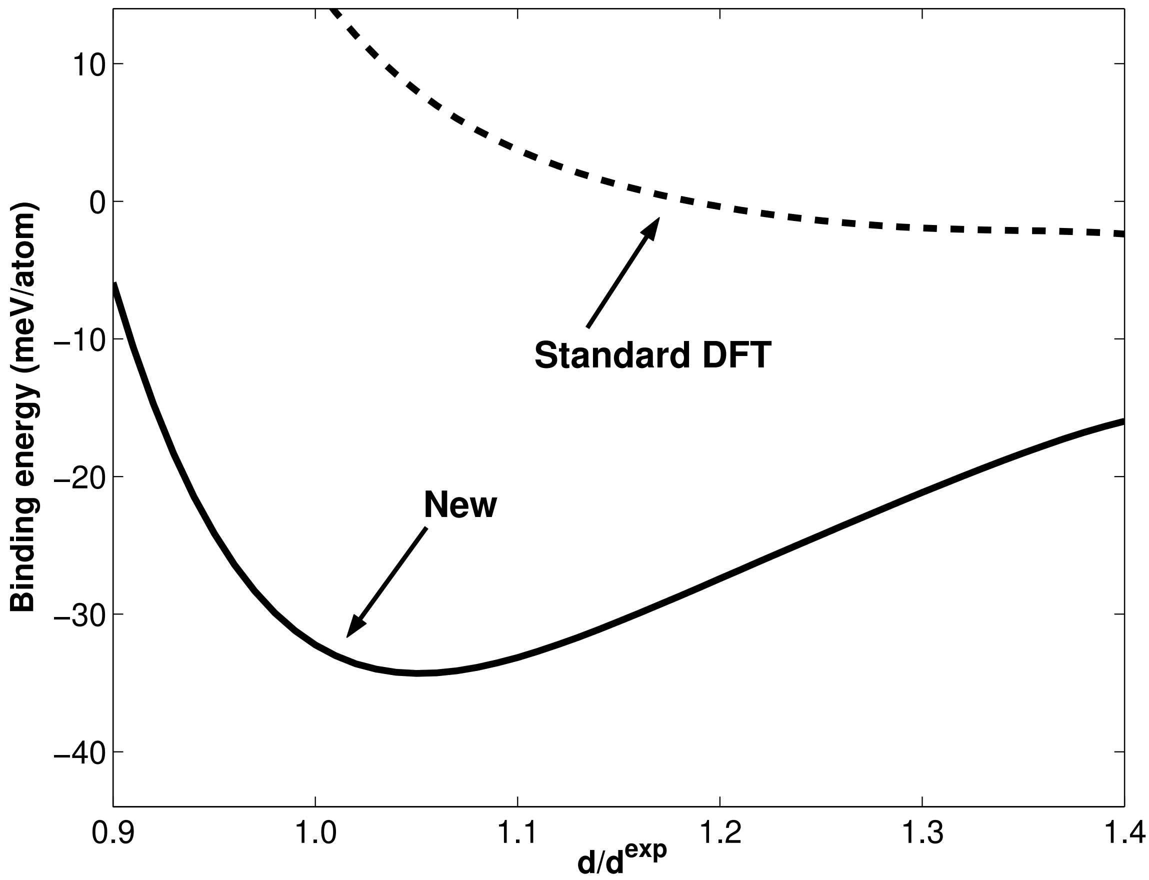

Figure 2: The binding energy of a single graphene-graphene pair as a function of interplanar separation (d), presented in units of a periodic (graphite) system. A pseudopotential code [31] and a semilocal approximation [32] are used to calculate the standard-DFT electron densities, $n_d(\mathbf{r})$, and energies, for each separation d. The exchange part of the new functional is unchanged from standard DFT, while the correlation part [1] is easily related to it. The standard correlation functional can be written as $E_{\rm c}^{\rm standard} = E_{\rm c}^{\rm LDA} + E_{\rm c}^{\rm semilocal}$ where $E_{\rm c}^{\rm LDA}$ is the old-standard or local-density approximation [33] contribution and $E_{\rm c}^{\rm semilocal}$ is the semilocal correction. Correspondingly, our new correlation functional [34] may be written $E_{\rm c}^{\rm new} = E_{\rm c}^{\rm LDA} + E_{\rm c}^{\rm nonlocal}$, where $E_{\rm c}^{\rm nonlocal}$ is our replacement, which although fully nonlocal, is calculationally inexpensive. It is calculated using Eqs. (9), (19) and (23) of Ref. [1] with laterally averaged densities $n_d(z)$ as input (The relevant density is out in the tails of the electron density of each layer [35]. It is smooth, making the corrugation negligible compared with the separation between the fragments). The system-specific component ($q_\perp$) is kept fixed for all separations d. It is determined by comparing a (standard DFT) calculation of the static polarizability (actually α_{zz}, where the z direction is perpendicular to the graphene plane) of a single graphene sheet to the classical electrodynamic formulation.

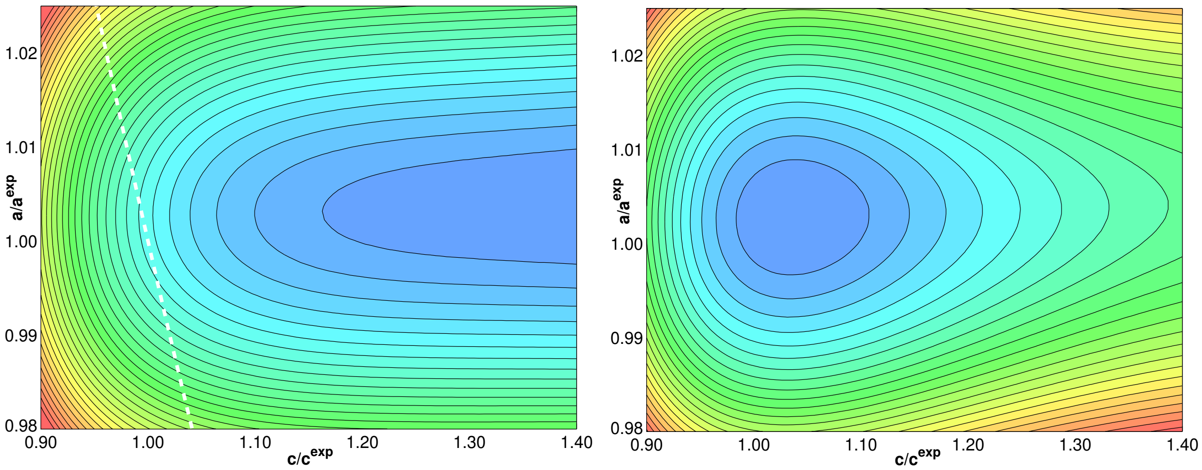

Figure 3: *Left panel:* Total-energy contour plot for graphite in the c–a plane, calculated with standard DFT. The energy is increasing in order darker to lighter shades of grey with a 10 meV contour spacing. The lattice parameters are defined in Fig. 1. An all-electron projector augmented-wave method [36] and a semilocal approximation [32] are used. The dashed curve is the locus of points giving the experimental volume; it illustrates that a calculation so constrained will fortuitously give the correct values of c and a [37] *Right panel:* Same system calculated with our nonlocal-correlation corrected DFT, as described in Fig. 2.

TABLES

Table 1. Calculated properties of graphite, compared to experimental data. The table shows the geometry (a, c), binding energy (E_0) and bulk modulus (B_0) obtained with the early-standard DFT, the current-standard DFT, and our revised DFT.

Method	a [Å]	c [Å]	E_0 [meV/at]	B_0 [GPa]
Early DFT (LDA)	2.45	6.6	20^a	51
Standard DFT (GGA)	2.47	$\gg 7.5$	~ 5	~ 7
Revised DFT (Ref. [1])	2.47	7.0	34	33
Exp.	2.46	6.7	35 ± 10^b	33^c

^{a} Ref. [26]. ^{b} Ref. [18]. ^{c} Ref. [30].